Front. Electr. Electron. Eng. China 2009, 4(2): 205–209
DOI 10.1007/s11460-009-0036-8

RESEARCH ARTICLE

Fang HE, Zhengyu ZHAO

Characteristics of high frequency radio wave propagated in heated ionospheric regions

Abstract A two-dimensional Ohm heating theoretic model in the magnetizing ionosphere and a ray-tracing model in a discrete ionosphere background are used to analyze quantitatively the characteristics (mainly the Doppler shift and the phase shift) of the over-the-horizon radar (OTHR) wave, which propagates through the ionospheric region heated by high frequency radio wave. The simulation results about the Doppler and the phase shift are obtained within two minutes after the heater is on. Preliminary conclusions are given by comparing the numerical results with experimental data.

Keywords over-the-horizon radar (OTHR), wave characteristics, Doppler shift, phase shift

1 Introduction

Since the 1980s, Norway, Sweden and Finland had started using the over-the-horizon radar (OTHR) to diagnose the ionospheric region heated by high frequency radio wave [1] in order to find the change of characteristics of high frequency radio wave propagated in heated ionospheric regions. Because this kind of diagnostic experiment is expensive and region dependent [2,3], numerical simulation becomes a convenient way to predict and evaluate the experiment results.

The theory and numerical simulation of the ionosphere heated by high frequency radio wave have been well developed. The first ground-based artificial ionosphere heating experiment was led by Utlaut, in April 1970 in Platteville, USA [4,5]. However, the theory of ground-based artificial ionospheric modification had been developed in the 1950s. DuBois, Silin, Nishikawa, Perkins found two main heating mechanisms [6–9]: Ohmic heating and parametric instability. Lots of domestic researchers are studying the numerical model of the heating experiment. Huang Wengeng developed the model of lower ionosphere heating and higher ionosphere heating [10,11], Ni Binbin developed a one-dimensional unmagnetized ionosphere heating model [12] and a two-dimensional model [13]. Because the one-dimensional model is a function of altitude only, the grads of electron density (ED) in the horizontal direction cannot be expressed. However the ED horizontal grads can affect the radio wave propagation in the ionosphere greatly [14,15], when the ionosphere ED is given in two dimensions, ray-tracing program in the numerical way has to be used [16].

As to the numerical way of ray-tracing program, there are many researchers who have studied this subject. In view of the computational complexity of a ray-tracing program, analytic ray-tracing methods are used. However, the two-dimensional ionosphere model cannot be expressed in an analytic way. Xie Shuguo has developed a grid method for a ray-tracing program under two-dimensional ionosphere background [16]. It divides the ionosphere background into a series of grids where the ED grads is a constant. In this way, the ray-tracing program can be run effectively with good accuracy.

Based on the two-dimensional magnetized ionosphere Ohmic heating model and the discrete ED ray-tracing program, simulation on the OTHR diagnostic wave in the heated ionosphere region is carried on. The results are helpful to predict the influence of artificial ionosphere heating experiment to the characteristics of diagnostic wave which propagates through the ionosphere.

2 Model descriptions

2.1 Two-dimensional magnetized ionosphere heating model

As to the two-dimensional magnetized ionosphere heating model, Ni Binbin [13] has already fully elaborated on it. The relative functions are:

Translated from *Chinese Journal of Radio Science*, 2008, 23(3): 466–470 [译自: 电波科学学报]

Fang HE, Zhengyu ZHAO (✉)
School of Electronic Information, Wuhan University, Wuhan 430072, China
E-mail: Dicilab@yahoo.com.cn

Momentum equation of two-dimensional ionosphere background:

$$n_e v_e = Dk_B\left\{\frac{1}{\sin\lambda}\frac{\partial}{\partial z}[n_e(T_e+T_i)] + \frac{1}{\cos\lambda}\frac{\partial}{\partial x}[n_e(T_e+T_i)]\right\} + Dg\sin\lambda\sum_\alpha(m_\alpha n_\alpha); \quad (1)$$

Continuity equation of various charged particles:

$$\frac{\partial n_\alpha}{\partial t} - \frac{1}{\sin\lambda}\frac{\partial}{\partial z}(n_\alpha v_\alpha) - \frac{1}{\cos\lambda}\frac{\partial}{\partial x}(n_\alpha v_\alpha) = \beta_\alpha(x,z,t) + P_\alpha(x,z,t) + S_{o\alpha}(x,z); \quad (2)$$

Energy equation of electron temperature:

$$\frac{\partial T_e}{\partial t} - v_e\left(\frac{1}{\sin\lambda}\frac{\partial T_e}{\partial z} + \frac{1}{\cos\lambda}\frac{\partial T_e}{\partial x}\right) - \frac{2T_e}{3}\left(\frac{1}{\sin\lambda}\frac{\partial v_e}{\partial z} + \frac{1}{\cos\lambda}\frac{\partial v_e}{\partial x}\right) - \frac{2\kappa_e}{3n_e k_B}\left(\frac{1}{\sin^2\lambda}\frac{\partial^2 T_e}{\partial z^2} + \frac{1}{\cos^2\lambda}\frac{\partial^2 T_e}{\partial x^2} + \frac{2}{\sin\lambda\cos\lambda}\frac{\partial^2 T_e}{\partial x\partial z}\right) = \frac{2(Q_{HF}+Q_0-L_e)}{3n_e k_B}, \quad (3)$$

where k_B is Boltzmann's constant, κ_e is electron conductivity coefficient, λ is the angle between geomagnetic field and horizontal direction, n_e is electron density, v_e is electron velocity, n_α represents the density of one kind of particle, v_α represents the velocity of one kind of particle, T_e and T_i represent electron and ions temperature respectively, g is the acceleration of gravity, D is diffusion coefficient, $S_{o\alpha}$ represents the stationary source which keeps one kind of particle, P_α and β_α represent generation rate and recombination rate of one kind of particle respectively, Q_{HF} is the ionosphere absorption term, Q_0 is the radiant energy of solar power which keeps the homeostasis of electron temperature, L_e is the cooling rate of electron energy.

It has to be noticed that the initial ionosphere is modeled by International Reference Ionosphere-2001 (IRI-2001), and is considered as horizontal homogeneous stratified.

2.2 Ray-tracing in discrete ionosphere background

The vertical range of initial ionosphere background is 60–400 km, step length is 1 km; the horizontal range is 0–3000 km, step length is 1 km. Then we get a 341×3001 space grid.

The heating region is represented by a 41×255 space grid.

The relation of heating region and the initial ionosphere background is shown in Fig. 1.

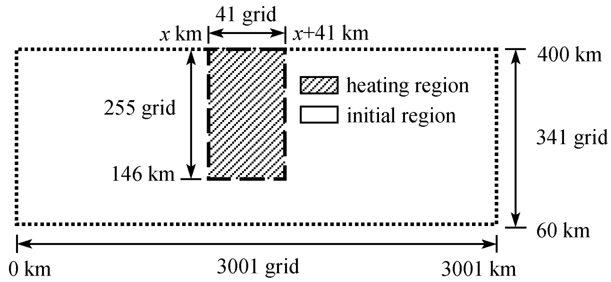

Fig. 1 Heated ionosphere background grid graph

3 Parameters

3.1 Heating parameters

The ionosphere background model is determined by the IRI-2001. The location of interest is at the city of Dongfang in Hainan province (19.0°N, 108.7°E, geomagnetic inclination: 24.6°).

1) Effective radiation power (ERP): 10 MW.
2) Heating wave frequency: f_h= 6 MHz.
3) Heating time: local time 20:00, Sep 15th, 2006.
4) Heating duration: 120 s.
5) Heating step length: 10 s.
6) Altitude range of heating: 146–400 km.

3.2 Ray-tracing parameters

The ray-tracing model is described in Sect. 2.2. The distance between the center of the heating region and the diagnostic wave transmitter is 440 km. The diagnostic wave parameters are:

1) Diagnostic wave frequency: f= 11 MHz.
2) Elevation angle θ: 50°, 51°, 52°, 53°, 54°, 55°.

The geometric relation of ray-tracing and heating region is shown in Fig. 2, where Tx, Rx and 'heater' represent the location of the transmitter, the receiver and the heating facility, respectively. The shaded parts represent the heated ionosphere region.

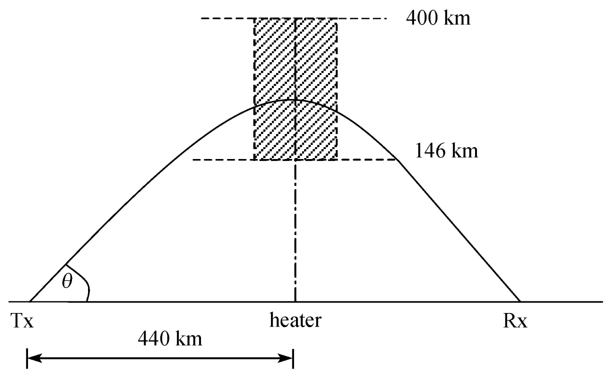

Fig. 2 Ray path of diagnostic wave in heated ionosphere

4 Simulation results of diagnostic wave

Neglecting the influence of magnetic field, the Appleton-Hartree formula can be written as

$$\mu^2 = 1 - X, \tag{4}$$

where μ is the refractive index, $X = \omega_N^2/\omega^2 = e^2N/(\varepsilon_0 m\omega^2)$; e, m and ε_0 are the value of electron charge and mass, and dielectric constant in free space, respectively. N is the electron density. Thus,

$$\mu = \sqrt{1-X} = \sqrt{1-\frac{e^2N}{\varepsilon_0 m\omega^2}}. \tag{5}$$

The change of phase path caused by ionosphere is [17]

$$\Delta l_{\mathrm{p}} = \int_s (\mu - 1)\mathrm{d}l = -\int_s \left(1-\sqrt{1-\frac{e^2N}{\varepsilon_0 m\omega^2}}\right)\mathrm{d}l, \tag{6}$$

where N is the function of propagation path.

The phase refractive index in ionosphere is less than 1, so the wave phase advance may occur. When the phase distortion caused by irregularities in the ionosphere less than Fresnel radius is comparable to 1 radian, the amplitude scintillation may occur [17]. Phase advance can be written as

$$\Delta\phi = \frac{2\pi}{\lambda}|\Delta l_{\mathrm{p}}| = \frac{2\pi}{\lambda}\int_s \left(1-\sqrt{1-\frac{e^2N}{\varepsilon_0 m\omega^2}}\right)\mathrm{d}l. \tag{7}$$

Equation (7) shows that the phase change is proportional to total electron content (TEC). Any changes with time can result in the phase change, and this phase change with time means the frequency disturbance in the received signal, which is Doppler shift. The Doppler shift caused by ionosphere disturbance is [18]

$$\Delta f_d = \frac{1}{2\pi}\frac{\mathrm{d}(\Delta\phi)}{\mathrm{d}t} = \frac{1}{\lambda}\frac{\mathrm{d}|\Delta l_{\mathrm{p}}|}{\mathrm{d}t} = \frac{1}{\lambda}\frac{\mathrm{d}\left[\int_s \left(1-\sqrt{1-\frac{e^2N}{\varepsilon_0 m\omega^2}}\right)\mathrm{d}l\right]}{\mathrm{d}t}, \tag{8}$$

where λ is the diagnostic wave length.

Based on the ray path calculated by Sect. 2.1 and heated ionosphere background in Sect. 2.2, the change of phase path Δl_{p} can be obtained, from which Doppler shift of single-pass can be obtained.

Figures 3 and 4 show the simulation results of Doppler shift and phase shift of OTHR diagnostic wave varied with the heating duration. The heating and diagnostic wave parameters are given in Sects. 3.1 and 3.2. The variform dots in the figures represent the results with different elevation angle.

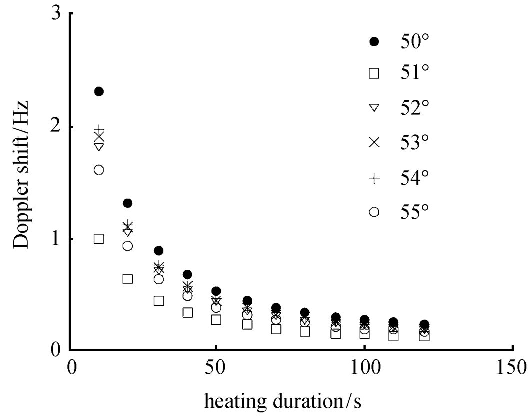

Fig. 3 Doppler shift vary with heating duration

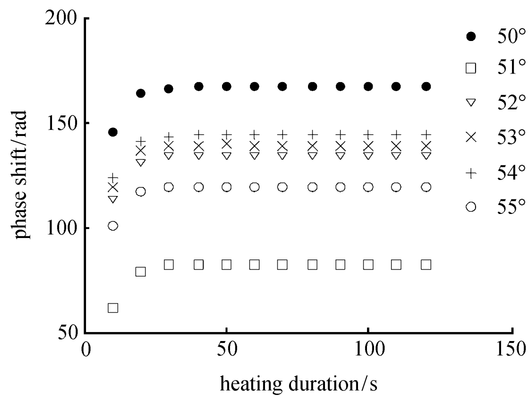

Fig. 4 Phase shift vary with heating duration

As shown by the dotted line in Fig. 3, the Doppler shift of 6 simulation diagnostic waves has the similar trend. In less than 10 s from when the heater is turned on, Doppler shift increases to about 2 Hz. With the time passing, Doppler shift decreases using the time axis as an asymptote. The Doppler shift of all 6 diagnostic waves reduces to 0.3 Hz after the heater is turned on for 120 s. This suggests that the change of the density variation is stabilizing, and the heating effect is close to saturation. The dotted lines in Fig. 4 increase to the saturated level in 30 s after the heater is on, with small disturbance in the latter 90 s.

It has to be emphasized that as shown in Fig. 2, only the single path effects of the diagnostic wave is considered in order to make the comparison of the simulation results convenient.

5 Analyze on experimental results with simulation results

In October 1980, the ionosphere heated by high frequency (HF) wave experiment was held by Norway, Sweden and

Finland in Tromsø, and the diagnostic wave was used for analysis [1].

5.1 Doppler shift of diagnostic wave

The Doppler shift of diagnostic wave passing through the heated ionosphere region in Tromsø is shown in Fig. 5. The fundamental frequency of the 3 diagnostic waves is 3.498 MHz, and offset frequencies for each wave are 2 Hz, 5 Hz and 9 Hz respectively. The tag 'ON' and 'OFF' indicates the heater state. The abscissa represents the universal time, and the duration of heater on and off is both 2 min. In Fig. 5, before the heater is turned on, the Doppler shift of 3 diagnostic waves had no significant change. From the time the heater is turned on, Doppler shift had a significant increase of 1.5–2 Hz in the forward bias. These results are consistent with the simulation results in Fig. 3.

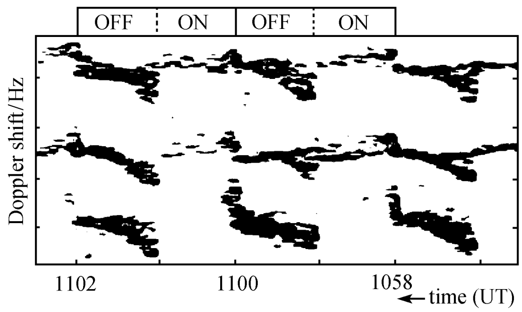

Fig. 5 Doppler shift of HF diagnostic waves passing through heated ionosphere region in Tromsø on Oct. 7th, 1980 [1]

5.2 Phase shift of diagnostic wave

Heater factor 'p' in Fig. 6 indicates the heater power of ERP$\times p$ MW. The heater power in 0–2 min, 4–6 min, 8–10 min, 12–14 min is 160 MW, 80 MW, 40 MW, 20 MW, respectively. Because the given simulation results are calculated with the heater power of 160 MW, only the condition of $p = 1$ is considered.

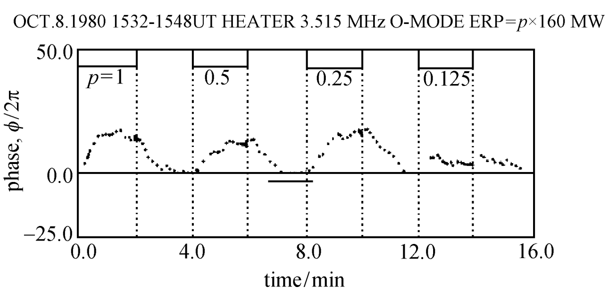

Fig. 6 Phase shift of HF diagnostic wave of 3.778 MHz passing through heated ionosphere region in Tromsø on Oct. 8th, 1980 [1]

In Fig. 7, within 2 min after the heater is turned on, the phase shift of diagnostic wave increased from 0 to 40π rad in 40 s, and the change in the latter 80 s was not significant. It suggests that the simulation analysis is consistent with the experiment results.

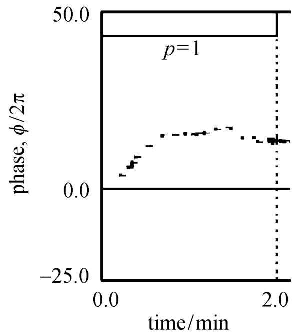

Fig. 7 Phase shift varies with heating duration when $p = 1$ [1]

6 Conclusions

1) The ground based high power radio wave can modulate the density or other parameters of a charged particle. These effects can influence the characteristics of OTHR waves which pass through the ionosphere.

2) Heating duration is a key parameter which determines the characteristics of diagnostic waves. With the increase of heating duration, the Doppler shift decreases.

3) The heating region has a saturation effect to the HF wave. It is concluded that after 1 min from when the heater turns on, the ionosphere reaches a saturation state.

References

1. Robinson T R. The heating of the high latitude ionosphere by high power radio waves. Physics Reports, 1989, 179(2–3): 79–209
2. Fejer J A, Gonzales C A, Ierkic H M, Sulzer M P, Tepley C A, Duncan L M, Djuth F T, Ganguly S, Gordon W E. Ionospheric modification experiments with the Arecibo heating facility. Journal of Atmospheric and Terrestrial Physics, 1985, 47(12): 1165–1179
3. Kohl H, Kopka H, Stubbe P, Rietveld M T. Introduction to ionospheric heating experiments at Tromsø — II: scientific problems. Journal of Atmospheric and Terrestrial Physics, 1993, 55(4–5): 601–603
4. Carroll J C, Violette E J, Utlaut W F. The Platteville high power facility. Radio Science, 1974, 9(11): 889–894
5. Utlaut W F. An ionospheric modification experiment using very high power, high frequency transmission. Journal of Geophysical Research, 1970, 75(31): 6402–6405
6. DuBois D F, Goldman M V. Radiation induced instability of electron plasma oscillations. Physical Review Letters, 1965, 14(14): 544–546
7. Silin V P. Anomalous nonlinear dissipation of high frequency radio waves in plasma. Soviet Physics Uspekhi, 1973, 15(6): 742–758
8. Nishikawa K. Parametric excitation of coupled waves — I: general

formulation. Journal of the Physical Society of Japan, 1968, 24(4): 916–922
9. Gurevich A V. Nonlinear Phenomena in the Ionosphere. New York: Springer-Verlag, 1978
10. Huang Wengeng, Gu Shifen. Interaction between the powerful high-frequency radio wave and the lower terrestrial ionosphere. Chinese Journal of Space Science, 2003, 23(3): 181–188 (in Chinese)
11. Huang Wengeng, Gu Shifen. The heating of upper ionosphere by powerful high-frequency radio waves. Chinese Journal of Space Science, 2003, 23(5): 343–351 (in Chinese)
12. Ni Binbin, Zhao Zhengyu, Xiang Wei, Wei Hanying. Numerical modeling of ionospheric modification with powerful HF pump waves. Chinese Journal of Radio Science, 2004, 19(3): 274–279 (in Chinese)
13. Ni Binbin. Theoretical and numerical studies on ionospheric modification caused by incidence of high-power high-frequency radio waves. Dissertation for the Doctoral Degree. Wuhan: Wuhan University, 2005 (in Chinese)
14. Fridman O V, Fridman S V. A method of determining horizontal structure of the ionosphere from backscatter ionograms. Journal of Atmospheric and Terrestrial Physics, 1994, 56(1): 115–131
15. Russell C J, Dyson P L, Houminer Z, Bennett J A, Li L. The effect of large-scale ionospheric gradients on backscatter ionograms. Radio Science, 1997, 32(5): 1881–1897
16. Xie Shuguo. A study on the ionospheric parameter inversion of backscatter ionograms. Dissertation for the Doctoral Degree. Wuhan: Wuhan University, 2001 (in Chinese)
17. Lawrence R S, Little C G, Chivers H J. A survey of ionospheric effects upon earth-space radio propagation. Proceedings of the IEEE, 1964, 52(1): 4–27
18. Budden K G. The Propagation of Radio Waves. Cambridge: Cambridge University Press, 1985